

Ontogenic Identification and Analysis of Mesenchymal Stromal Cell Populations during Mouse Limb and Long Bone Development

Gretel Nusspaumer,^{1,5} Sumit Jaiswal,^{1,5} Andrea Barbero,² Robert Reinhardt,¹ Dana Ishay Ronen,³ Alexander Haumer,² Thomas Lufkin,⁴ Ivan Martin,² and Rolf Zeller^{1,*}

¹Developmental Genetics, Department Biomedicine, University of Basel, 4058 Basel, Switzerland

²Tissue Engineering Group, Department of Biomedicine, University of Basel and University Hospital Basel, 4056 Basel, Switzerland

³Tumor Biology, Department Biomedicine, University of Basel, 4058 Basel, Switzerland

⁴Department of Biology, Clarkson University, Potsdam, NY 13699, USA

⁵Co-first author

*Correspondence: rolf.zeller@unibas.ch

<http://dx.doi.org/10.1016/j.stemcr.2017.08.007>

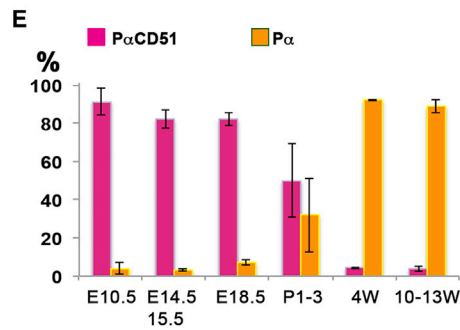
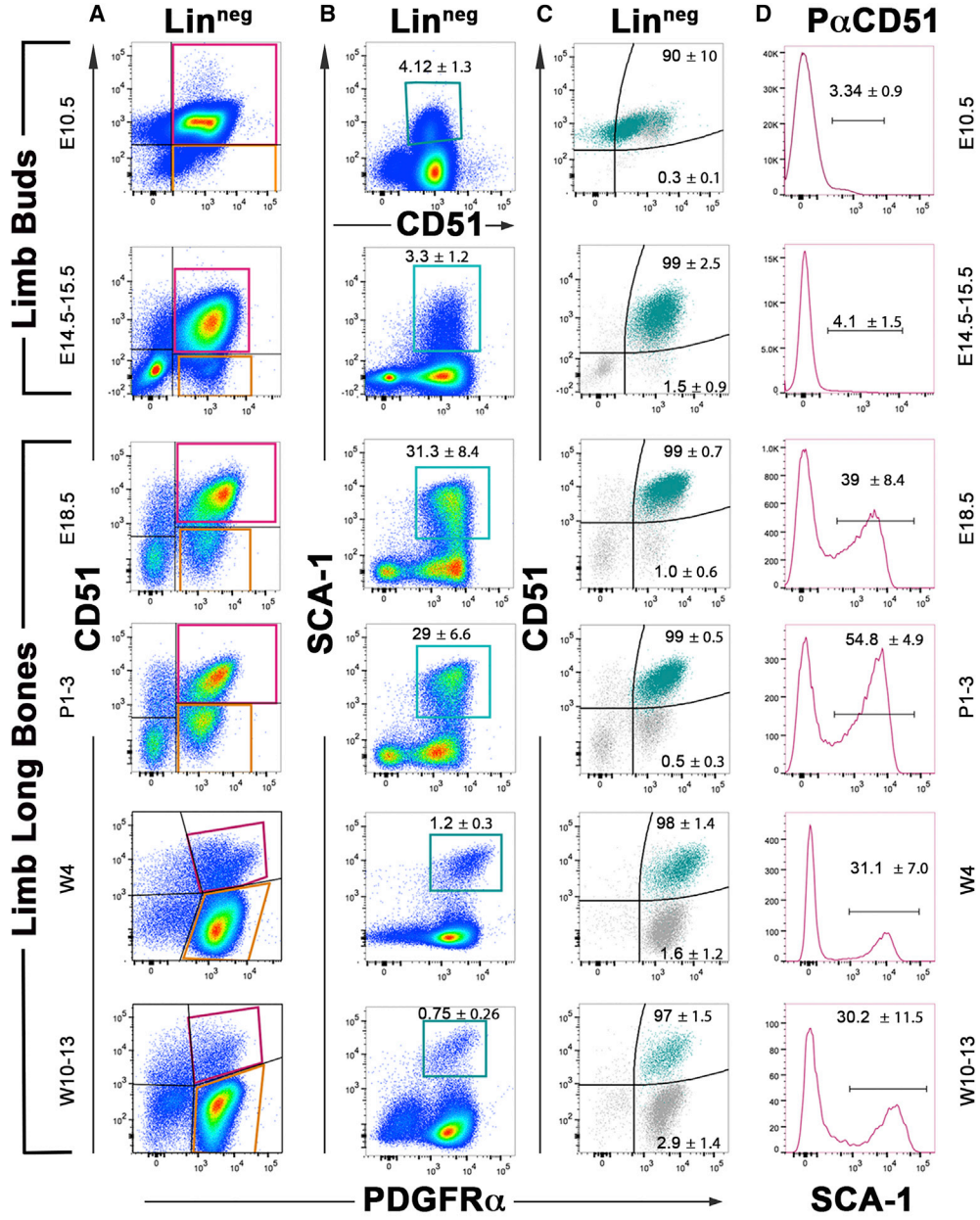
SUMMARY

Bone-derived mesenchymal stromal cells (MSCs) differentiate into multiple lineages including chondro- and osteogenic fates and function in establishing the hematopoietic compartment of the bone marrow. Here, we analyze the emergence of different MSC types during mouse limb and long bone development. In particular, PDGFR α ^{POS}SCA-1^{POS} (P α S) cells and mouse skeletal stem cells (mSSCs) are detected within the PDGFR α ^{POS}CD51^{POS} (P α CD51) mesenchymal progenitors, which are the most abundant progenitors in early limb buds and developing long bones until birth. Long-bone-derived P α S cells and mSSCs are most prevalent in newborn mice, and molecular analysis shows that they constitute distinct progenitor populations from the earliest stages onward. Differential expression of CD90 and CD73 identifies four P α S subpopulations that display distinct chondro- and osteogenic differentiation potentials. Finally, we show that cartilage constructs generated from CD90^{POS} P α S cells are remodeled into bone organoids encompassing functional endothelial and hematopoietic compartments, which makes these cells suited for bone tissue engineering.

INTRODUCTION

A wealth of studies using bone-derived mesenchymal stromal cells (MSCs) has revealed their importance for engineering to repair cartilage and bone tissues, and for ameliorating hematopoietic disorders (Bianco, 2014). However, it is still not firmly established whether MSC populations encompass mesenchymal progenitor and/or stem cells. In a recent review, Caplan (2017) proposes that MSCs, rather than being progenitor/stem cells, home to sites of injury and secrete factors that induce regeneration by resident stem cells. As it is indeed difficult to expand MSCs in culture without affecting their initial characteristics (Bianco, 2014; Mabuchi et al., 2013), the prospective isolation and direct analysis of primary mesenchymal progenitors from human bone marrow and mouse long bones is central to identify their origins and assessing their multi-lineage differentiation potential. Since the first isolation of clonogenic mesenchymal progenitors from human bone marrow (Sacchetti et al., 2007), lineage tracing and prospective characterization using mouse models has identified different types of mesenchymal progenitor/stem cells and provided fundamental insights into their functions during normal bone homeostasis and repair (Morrison and Scadden, 2014; Ono and Kronenberg, 2016). However, the relatedness of these different mesenchymal populations from mice and their corresponding human orthologs remains uncertain.

Studying mouse limb development provides insight into the ontology and functions of the mesenchymal progenitors that orchestrate development of long bones (reviewed by Long and Ornitz, 2013). In brief, the development of the skeletal primordia in early mouse limb buds is initiated by the condensation of multipotent mesenchymal progenitors at around embryonic day 10.5 (E10.5) and their commitment as *Sox9*-expressing osteo-chondrogenic progenitors (Akiyama et al., 2005), which will form the cartilage primordia. The SOX9-positive cells differentiate into proliferating chondrocytes while peripheral mesenchymal cells will form the perichondrium (Akiyama and Lefebvre, 2011). Endochondral ossification is initiated after chondrocytes become hypertrophic (~E12.5), which involves differentiation of perichondrium progenitors into *Osterix* (*Osx*) expressing osteoblastic and mesenchymal progenitors (Liu et al., 2013; Maes et al., 2010; Mizoguchi et al., 2014; Ono et al., 2014a). Limb long bone growth and bone marrow formation depends on angiogenesis, which is triggered by vascular endothelial growth factor (VEGF)-mediated attraction of endothelial and hematopoietic progenitors (\geq E14.5; Morrison and Scadden, 2014). The main migration of hematopoietic stem cells (HSCs) from the fetal liver to the bone marrow initiates perinatally, peaks immediately after birth, and continues until puberty, after which bone homeostasis is achieved (Kim et al., 2007; Trumpp et al., 2010). Concurrently, the cellular composition of the mesenchymal stromal compartment changes to support hematopoiesis (Greenbaum et al., 2013; Maes et al.,



(legend on next page)



2010; Mizoguchi et al., 2014). Marking of *Col2a* expressing cells in mouse embryos at E13.5 shows that these cells are retained in the epiphysis and metaphysis of long bones for up to 1 year after birth (Ono et al., 2014b). Marking *Osx*-expressing cells at E14.5 allows detection of labeled descendants in the diaphysis of even older mice (Liu et al., 2013), which is not the case if *Osx*-positive hypertrophic chondrocytes are marked one day earlier (E13.5; Maes et al., 2010; Ono et al., 2014a). In addition to hypertrophic chondrocytes and early osteoblasts, *Osx* is expressed in mesenchymal progenitors of the developing bone marrow up to early postnatal stages (through postnatal day 3 [P3]; Mizoguchi et al., 2014; Ono et al., 2014b). These and other studies suggest that there are different checkpoints during the endochondral ossification program that dictate the induction or reprogramming of new types of mesenchymal progenitors *in situ* or from nearby tissues.

Prospective isolation by flow cytometry detecting specific signatures of cell-surface molecules allowed identification of distinct mesenchymal and skeletal progenitor populations. Among these is a rare population of cells isolated by enzymatic digestion of compact bone and referred to as P α S cells (CD45^{neg} TER119^{neg} PDGFR α ^{pos} SCA-1^{pos}; Morikawa et al., 2009). P α S cells are quiescent cells located in the perivascular space close to the endosteum. They display the highest fibroblast colony-forming units (CFU-F) capacity among the different mesenchymal progenitor populations isolated from mice and possess a robust tri-lineage differentiation potential (Morikawa et al., 2009; Zhou et al., 2014a). In mice, P α S cells give rise to osteoblasts, are able to maintain long-term HSCs, and home back to bone marrow following intravenous injection (Chan et al., 2009; Greenbaum et al., 2013; Hu et al., 2016; Morikawa et al., 2009; Park et al., 2012). P α S cells express *Mx1* but are not part of the cell populations marked in *Col2a* and *Osx* lineage-tracing experiments (Ono et al., 2014b; Park et al., 2012). More recently, CD200^{pos}CD51^{pos} mesenchymal progenitors (lacking CD90, CD105, and 6C3) were isolated as a mesenchymal population able to give rise to cartilage and bone. These mul-

tipotent cells were termed mouse skeletal stem cells (mSSCs) and are able to support hematopoiesis *in vivo* (Chan et al., 2015). Finally, analysis of bone marrow stromal cells from human fetuses identified a mesenchymal cell population expressing platelet-derived growth factor receptor α (PDGFR α) and CD51 (P α CD51 cells), which is also able to self-renew and support expansion of HSCs (Pinho et al., 2013).

As it is not clear when these different mesenchymal progenitor cells arise and to what extent they are ontogenetically related, we used their characteristic CD signatures for flow-cytometric analysis of the stromal compartment of limb buds and long bones from mouse embryonic and postnatal stages. We show that murine P α S cells and mSSCs, which arise among the P α CD51-positive mesenchymal cells in early limb buds, constitute two distinct cell populations in developing and adult long bones. P α S cells can be subdivided into four subpopulations using CD73 and CD90, which mark chondrogenic and osteogenic lineages, respectively (Chan et al., 2015; Chung et al., 2013; Ode et al., 2013; Wu et al., 2013). P α S cells are already detected during formation of the cartilage anlagen in early limb buds and are most abundant in newborn mice. We also determined the bone-forming capacity of cartilage engineered from CD90^{pos}, CD90^{neg} and parental P α S cells following subcutaneous implantation. The CD90^{pos} P α S scaffolds are efficiently remodeled into bone organoids (for a definition of bone organoids see Bianco, 2014), which contain a well-structured marrow consisting of mesenchymal progenitors and host-derived endothelial and hematopoietic compartments.

RESULTS

Ontogenic Identification and Relatedness of Limb Bud and Long Bone Mesenchymal Cell Populations with P α CD51 and P α S Signatures

Mouse limb buds and developing long bones were analyzed at different embryonic, fetal, and postnatal time points to

Figure 1. Ontogenic Identification of Mesenchymal Stromal Cells during Embryonic, Fetal, and Postnatal Limb Bud and Long Bone Development

(A–D) Cells isolated from total limb buds at embryonic day 10.5 (E10.5), long bones at E14.5–15.5, E18.5, postnatal days 1–3 (P1–3), week 4 (W4; juvenile stage), and W10–13 (adult stages) were analyzed by flow cytometry. The analysis was done from forelimb buds at E10.5 and hindlimb long bones at all subsequent stages. Red cell lysis was included for older stages (\geq W4). The lineage marker pool (Lin) includes the following antigens: CD45, TER119, CD31, Gr1, and CD11b (all stages) plus EpCAM and CD309 (only for limb buds). Dead cells were gated out using 7AAD. Results are shown as pseudo-color plot representations of the subsequent analysis of the lineage-negative (Lin^{neg}) fraction. (A and B) Distribution of Lin^{neg} cells expressing either the platelet-derived growth factor receptor α (PDGFR α)/CD51 or PDGFR α /SCA-1 antigens. Note that in limb buds at E10.5, CD51 is assessed against SCA-1 (B, see text). (C) Overlapping dot plot representations show that P α S cells (blue) are mostly contained in the P α CD51 population (gray). (D) Fraction of the SCA-1-positive P α CD51 cells corresponding to P α S cells.

(E) Percentage of P α CD51- and P α -positive cells in the Lin^{neg} population. Per stage $n \geq 3$ independent experiments were analyzed. All results are presented as averages \pm SD.



identify mesenchymal cells with signatures of different MSC populations. Following preparation of single-cell suspensions, dead cells, endothelial, hematopoietic, and epithelial/ectodermal cells were first removed using the appropriate cell-surface markers (see [Supplemental Experimental Procedures](#)). An ontogenetic flow-cytometric analysis was done using the remaining so-called lineage-negative (Lin^{neg}) cells from the different stages ([Figures 1 and 2](#)). Initially, the signatures of two types of MSC, namely $\text{P}\alpha\text{CD51}$ and $\text{P}\alpha\text{S}$ progenitors, were profiled ([Figure 1](#)). In developing mouse limb buds (E10.5 and E14.5–15.5), the vast majority of Lin^{neg} mesenchymal progenitors are $\text{P}\alpha\text{CD51}$ positive ($\sim 80\%$ – 95% , [Figures 1A and 1E](#)). During fetal long bone development (E14.5–18.5), $\text{P}\alpha\text{CD51}$ -positive cells (also including osteoblasts; [Chitteti et al., 2013](#)) remain most prominent ([Figure 1E](#), purple bars). During early postnatal development (P1–3), $\text{P}\alpha\text{CD51}$ cells account for $\sim 50\%$ of the Lin^{neg} cells, but their frequency drops to $\sim 4\%$ in juvenile and adult long bones. This decrease in $\text{P}\alpha\text{CD51}$ cells is paralleled by a significant increase in $\text{PDGFR}\alpha$ single-positive ($\text{P}\alpha$) cells after birth ([Figures 1A and 1E](#)).

In contrast to the predominant $\text{P}\alpha\text{CD51}$ population, $\text{P}\alpha\text{S}$ cells are less abundant ([Figure 1B](#)). In early limb buds (E10.5), SCA-1-positive mesenchymal progenitors express CD51 and intermediate levels of $\text{PDGFR}\alpha$ ([Figures 1B–1D](#)). From E14.5 onward, the $\text{P}\alpha\text{S}$ population increases progressively ([Figure 1C](#)) such that the highest proportion is observed around birth ($\sim 30\%$ at E18.5 and P1–3, [Figure 1B](#)). This analysis ([Figure 1](#)) establishes that the $\text{P}\alpha\text{CD51}$ -positive cells encompass the $\text{P}\alpha\text{S}$ population at all stages. This is relevant to potential therapeutic applications as, in contrast to CD51, the SCA-1 antigen is not present in humans ([Lee et al., 2013](#)).

$\text{P}\alpha\text{S}$ and mSSC Signatures Identify Two Distinct Progenitor Populations within the $\text{P}\alpha\text{CD51}$ Mesenchymal Cell Pool

We next analyzed the relationship between mSSC ($\text{CD51}^{\text{pos}}\text{CD200}^{\text{pos}}\text{CD90}^{\text{neg}}\text{CD105}^{\text{neg}}\text{6C3}^{\text{neg}}$ cells; [Chan et al., 2015](#)), $\text{P}\alpha\text{CD51}$, and $\text{P}\alpha\text{S}$ populations ([Figure 2](#)). Within the Lin^{neg} cells, CD51 is key to defining the predominant $\text{P}\alpha\text{CD51}$ population and SCA-1 identifies the $\text{P}\alpha\text{S}$ cells within this population ([Figure 2A](#)). In addition, the distribution of SCA-1- and CD200-positive cells within $\text{Lin}^{\text{neg}}\text{CD51}^{\text{pos}}$ cell pool was determined ([Figure 2B](#)). Strikingly, this analysis establishes that the $\text{SCA-1}^{\text{pos}}\text{P}\alpha\text{S}$ cells and $\text{CD200}^{\text{pos}}$ mSSCs segregate as mutually exclusive populations at all stages ([Figure 2B](#)). In early mouse limb buds (E10.5), the $\text{CD51}^{\text{pos}}\text{SCA-1}^{\text{pos}}\text{P}\alpha\text{S}$ cells are much more abundant than $\text{CD51}^{\text{pos}}\text{CD200}^{\text{pos}}$ cells (5% versus 0.5%; [Figures 2A, 2B, and 2E](#)). During fetal and early postnatal long bone development (E14.5–P2), $\text{P}\alpha\text{S}$ cells prevail over

mSSCs ([Figure 2E](#)). During peak bone angiogenesis and invasion of HSCs into long bones immediately after birth ([Trumpp et al., 2010](#)), $\text{P}\alpha\text{S}$ cells account for about half of all $\text{P}\alpha\text{CD51}$ cells. During puberty around week 4 (W4), mSSCs are about twice as frequent as $\text{P}\alpha\text{S}$ cells, while these populations are similarly represented in adult long bones ([Figures 2B and 2E](#)).

To gain insight into the potential overlap of these two cell populations with *Sox9*-positive progenitors, we included the *Sox9*^{RES-GFP} transgene in our analysis ([Chan et al., 2011](#)). In early limb buds (E10.5), the *Sox9*-GFP-positive cells correspond mostly to osteo-chondroprogenitors ([Akiyama et al., 2005](#) and our unpublished data). During subsequent development, *Sox9* is expressed by chondroblasts, reduced in proliferating chondrocytes, and re-expressed in pre-hypertrophic chondrocytes ([Akiyama et al., 2002](#); [Dy et al., 2012](#)). While *Sox9*-GFP levels are always low in $\text{P}\alpha\text{S}$ cells, the majority of mSSCs express intermediate to high levels of *Sox9* ([Figures 2C and 2D](#)).

As the *Prx1*-Cre transgene is expressed by most limb bud mesenchymal progenitors, we used it to activate a conditional GFP reporter (*β -ACTIN-loxP-stop-loxP-EGFP*; [Jagle et al., 2007](#); [Logan et al., 2002](#)). This allowed us to determine the fractions of $\text{P}\alpha\text{CD51}$, $\text{P}\alpha\text{S}$, and mSSC populations in GFP-positive cells at P2 ([Figure S1](#)). This analysis revealed that all GFP-positive cells are contained in the $\text{P}\alpha\text{CD51}$ population, which in turn shows that all $\text{P}\alpha\text{S}$ cells and mSSCs are GFP positive, i.e., are either *Prx1*-expressing cells or their descendants. In contrast the $\text{P}\alpha$ cells, which become predominant during postnatal development, are GFP negative ([Figure S1](#)). This analysis establishes $\text{P}\alpha\text{CD51}$ -positive cells as the major cell population within the mesenchymal (stromal) compartment during embryonic limb bud and fetal long bone development.

Next, the different mesenchymal populations in long bones after birth (P1–3) and during adult bone homeostasis (W10–13) ([Figure 3](#)) were analyzed for the expression of key genes relevant to chondrogenesis, osteogenesis, and hematopoiesis (*Prx1*, *Col2a1*, and *Mmp13*; *Osx*, *Lepr*, and *Cxcl12*, respectively). qRT-PCR analysis of the different mesenchymal populations ([Figure 3A](#)) showed that the different cell populations express distinct levels of these genes in a rather consistent manner when comparing newborn and adult mice. The most prominent Lin^{neg} population in adults, $\text{P}\alpha$ cells ([Figure 1B](#)), express none of these genes at birth and very variable levels of *Lepr* in adults ([Figures 3B and 3C](#)). Therefore, $\text{P}\alpha$ cells are unlikely to possess robust chondrogenic and osteogenic differentiation potential. $\text{P}\alpha\text{CD51}$ cells, $\text{P}\alpha\text{S}$ cells, and mSSCs express *Prx1* at birth and in adults. While $\text{P}\alpha\text{S}$ cells do not express chondrogenic and osteogenic markers, they express the highest levels of *Prx1* and low to intermediate levels of *Cxcl12* and *Lepr* at both stages ([Figures 3B and 3C](#)). This expression pattern

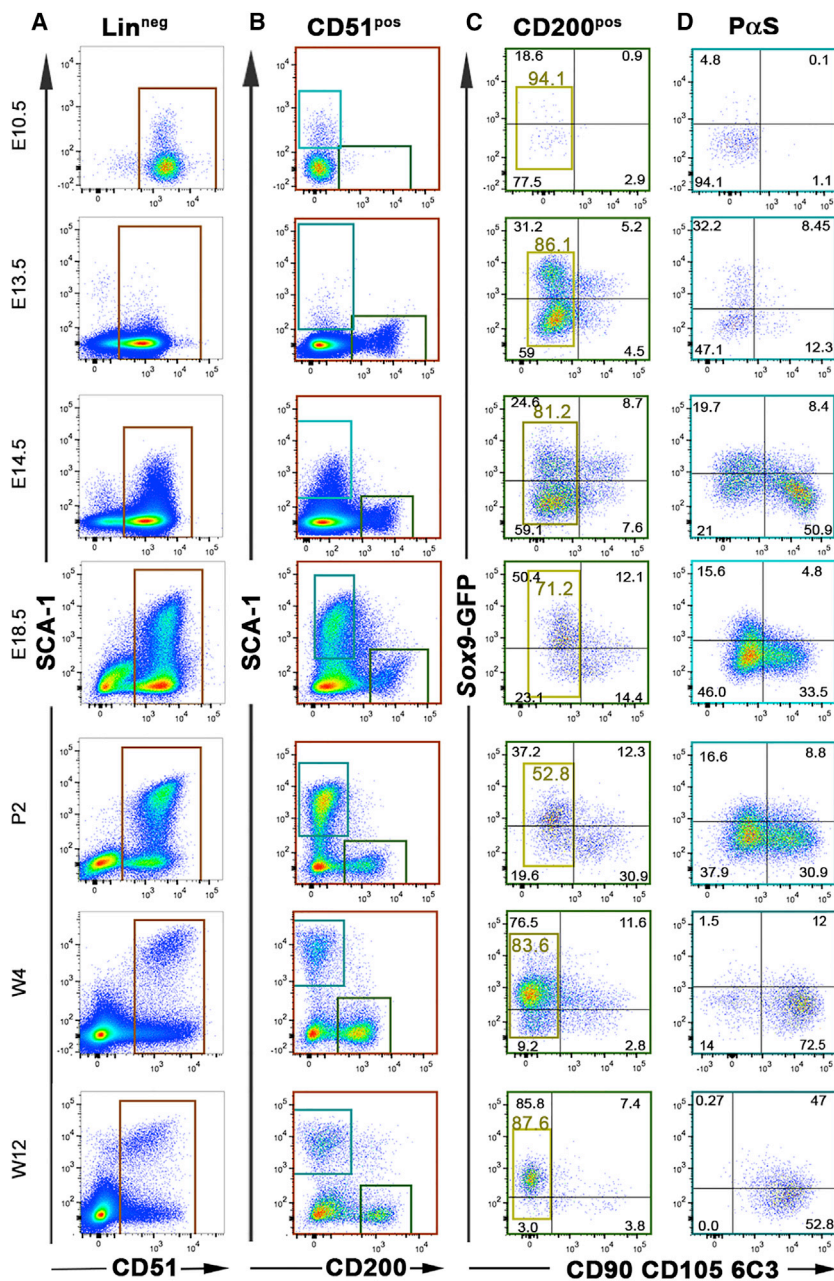


Figure 2. Ontogenic Analysis of Cells with mSSC and P α S Signatures

Flow-cytometric identification of different mesenchymal cell types in the Lin^{neg} fraction isolated from limb buds (E10.5–14.5) and limb long bones (E18.5–W12) of Sox9-GFP mice.

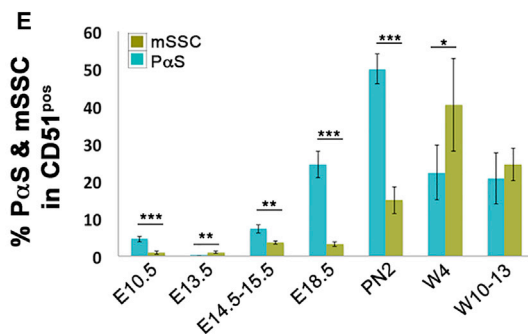
(A) Pseudo-color plot distribution of CD51- and SCA-1 positive Lin^{neg} cells. Note that the P α S cells are almost completely contained within the CD51^{pos}SCA-1^{pos} cell population.

(B) Analysis of CD51^{pos} Lin^{neg} cells with CD200 and SCA-1 shows that the CD200^{pos} (including mSSC) and SCA-1^{pos} cells (including P α S) define distinct cell populations at all stages.

(C) Additional flow-cytometric analysis identifies mSSCs as CD90^{neg}CD105^{neg}6C3^{neg} subpopulation within the CD51^{pos}CD200^{pos} fraction (percentage indicated within the yellow-green frame). Note that a significant fraction of mSSCs expresses Sox9-GFP from E13.5 and in particular from W4 onward.

(D) Variable expression of Sox9-GFP and the CD90, CD105, and 6C3 antigens in P α S cells.

(E) Graph showing the percentage of P α S cells and mSSCs in the Lin^{neg} CD51^{pos} population. Per time point and cell type $n \geq 3$ independent experiments were analyzed. All results are presented as averages \pm SD. Unpaired 2-tailed Student's t test was used to assess significance. * $p < 0.05$, ** $p < 0.01$, *** $p < 0.001$ were considered statistically significant.



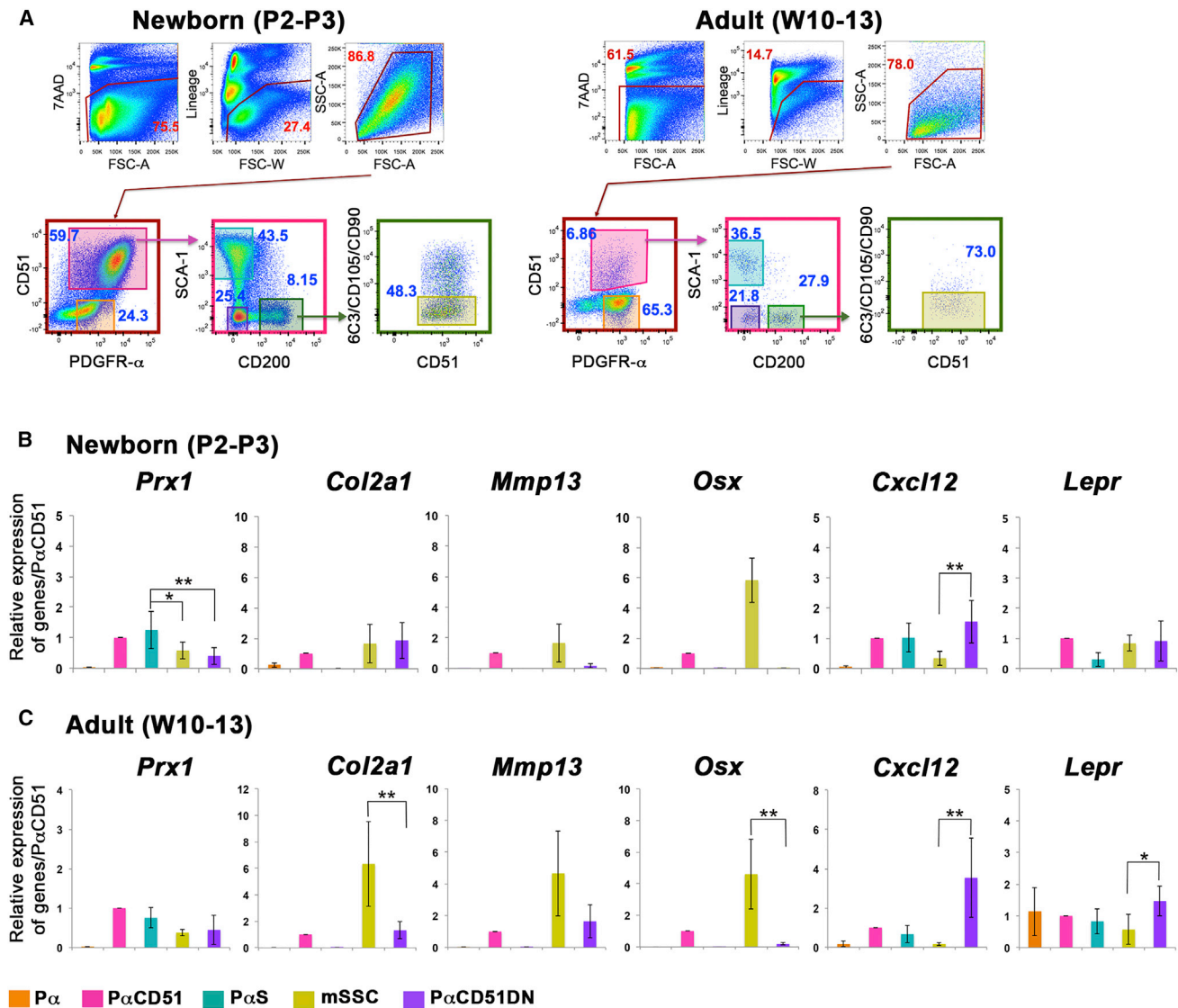


Figure 3. Differential Expression of Markers for Distinct Cell Lineages in the Isolated Mesenchymal Cell Populations

(A) Sorting strategy for the cells of interest isolated from hindlimb long bones (right). The color code for gates of the different populations is also the same for (B) and (C).

(B and C) qRT-PCR analysis of marker genes for different mesenchymal subpopulations in newborn (B) and adult mice (C). *Prx1* is expressed by limb mesenchymal progenitors; *Col2a1* by chondroblasts and primitive osteogenic progenitors; *Mmp13* by hypertrophic chondrocytes; *Osx* by pre- and hypertrophic chondrocytes, early osteoblasts, and MSC. *Cxcl12* and *Lepr* mark mesenchymal progenitors and MSC in the bone marrow. Expression levels are shown relative to the expression in $P\alpha$ CD51 cells. $n \geq 4$ independent experiments were analyzed per cell population. All results are presented as averages \pm SD. Unpaired 2-tailed Student's t test was used to assess significance. * $p \leq 0.05$, ** $p \leq 0.01$ were considered statistically significant.

points to the likely immature nature of $P\alpha$ S cells and is in agreement with their potential to support HSCs (see below). mSSCs isolated from adult long bones express high levels of *Col2a1*, *Mmp13*, and, notably, *Osx* (Figure 3C), which corroborates their osteo-chondrogenic potential (Chan et al., 2015). Finally, $SCA-1^{neg}CD200^{neg}P\alpha$ CD51 ($P\alpha$ CD51DN) cells express the highest levels of

Cxcl12 and *Lepr* while all other genes are expressed at only low to intermediate levels. These results indicate that the $P\alpha$ CD51DN population could encompass CAR cells (CXCL12-abundant reticular cells), which support B cell development (Greenbaum et al., 2013; Omatsu et al., 2010; Sugiyama et al., 2006). Taken together, this analysis of few selected key genes corroborates the distinct nature

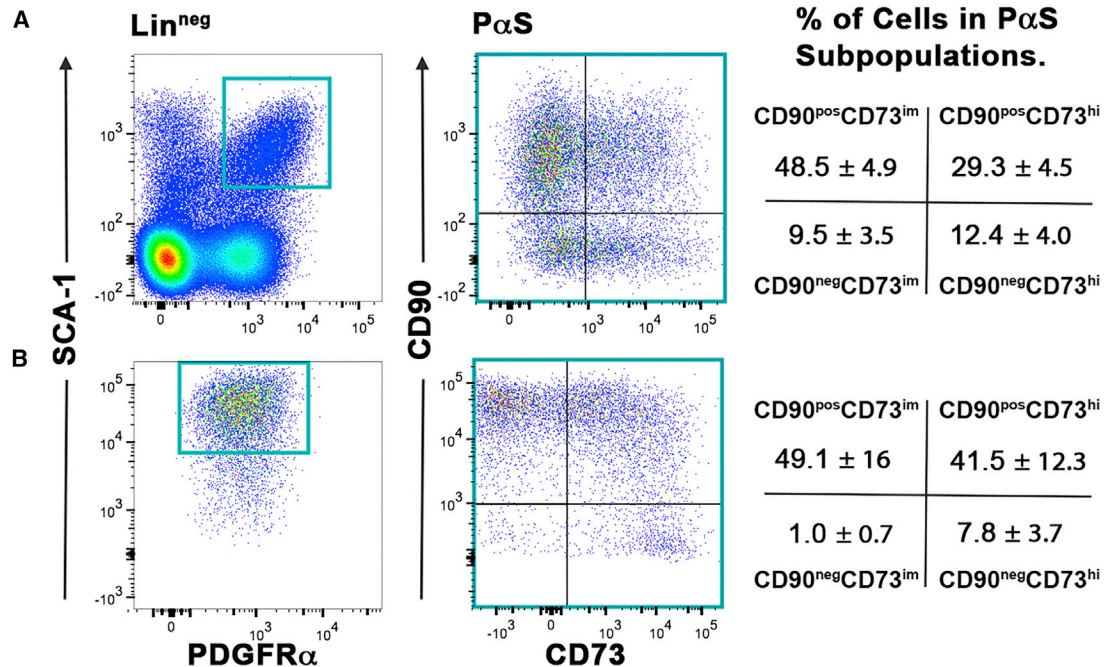


Figure 4. The PαS Populations Consist of Four Subpopulations Defined by Differential CD73 and CD90 Expression

(A) Flow-cytometric analysis of the expression of CD73 and CD90 in freshly isolated PαS cells from adult hindlimb long bones (W8–12). (B) Reanalysis of CD73 and CD90 subpopulations in PαS cells that have been expanded for two passages in culture. The rightmost panels show averages ± SD for n ≥ 8 independent experiments per dataset.

of the different mesenchymal stromal progenitor populations identified by flow cytometry.

PαS Cells Are a Heterogeneous Population Consisting of Subpopulations with Distinct CD Signatures

The PαS population was analyzed in more detail, as these cells are detected from early limb bud stages onward (see above). We performed the same analysis as shown in Figures 1 and 2 but also assessing the expression of CD73 and CD90 (Figure 4). CD73 is expressed by chondrocyte progenitors and CD90 marks the osteogenic lineage (see Introduction). Analysis of these two markers using freshly isolated adult PαS cells identifies four distinct subpopulations either negative or positive for CD90 and expressing intermediate (im) or high (hi) levels of CD73 (CD90^{neg}CD73^{im}, CD90^{neg}CD73^{hi}, and CD90^{pos}CD73^{im}, CD90^{pos}CD73^{hi}; Figure 4A). *In vitro* expansion of PαS cells causes a shift in the abundance of the four subpopulations. After two passages, the fractions of the two CD90^{neg} subpopulations are much reduced, while the CD90^{pos} PαS subpopulations become predominant (Figure 4B). This reduction is paralleled by a decrease in the multipotency, which affects mostly the osteo-chondrogenic differentiation potential (data not shown).

To understand when these four PαS subpopulations arise during limb long bone development, we analyzed Lin^{neg}

cells isolated from *Sox9*-GFP expressing embryos and mice by flow cytometry (Figure 5). During embryonic, fetal, and early postnatal stages, the *Sox9*-GFP-positive cells that mark the osteo-chondrogenic lineage (Figure 5A) comprise a significant fraction of all Lin^{neg} mesenchymal (stromal) cells (Figure 5E). From about 2 weeks postnatally, the fraction of *Sox9*-GFP cells within the Lin^{neg} fraction decreases significantly (Figures 5A and 5E). Concurrently, there is a switch in the proportions of the CD90^{neg} and CD90^{pos} PαS subpopulations (Figures 5E and 5F).

Mesenchymal SCA-1^{pos} cells in early limb buds express CD51 and intermediate levels of PDGFRα (E10.5; Figure 5B, compare with Figures 1 and 2). At this stage, *Sca-1* is expressed by the undifferentiated mesenchymal progenitors located distally and close to the limb bud ectoderm (Figure S2A; ten Berge et al., 2008). Furthermore, PαS cells express intermediate levels of CD73 (CD73^{im}) while CD90 is not detected (E10.5; Figures 5B, 5C, and S2B). The PαS progenitors are a heterogeneous population, as 10%–15% of them are also *Sox9*-GFP positive in early limb buds (Figure 5D). In fact, the majority of *Sox9*-GFP-positive progenitors in the stromal fraction correspond to osteo-chondrogenic progenitors that also express CD73 (Figure S2B). During the onset of endochondral ossification (E14.5–15.5), the four PαS subpopulations detected in adult long bones become apparent (Figures 5C and 5E, compare

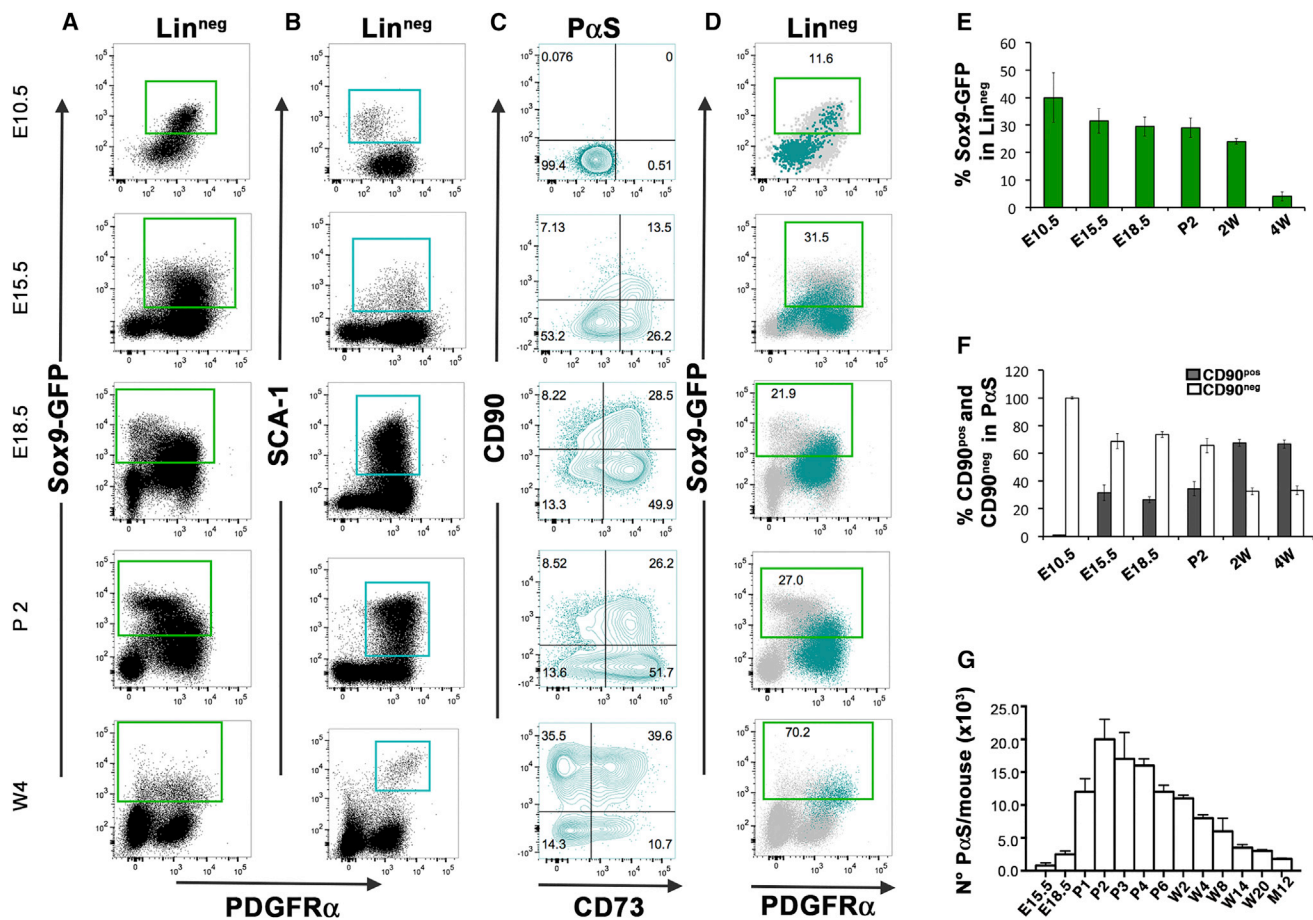


Figure 5. Developmental Origin of the PαS Subpopulations

(A–D) Flow-cytometric analysis of Lin^{neg} cells isolated from limb buds and long bones of Sox9-GFP mice. (A) Expression of Sox9-GFP in comparison with PDGFRα levels (gating frame indicates GFP-positive cells). (B) PαS cells are indicated by the gating frame in blue. (C) Contour plot analysis of PαS cells in combination with CD90 and CD73 reveals that the four subpopulations arise progressively during long bone development. (D) Overlap of PαS cells (turquoise) with Sox9-GFP-positive cells (gray, from A). The gating frame shows the fraction (%) of Sox9-expressing PαS cells.

(E) Percentage of Sox9-GFP-positive cells in the Lin^{neg} population.

(F) Percentage of CD90^{neg} (white bars) and CD90^{pos} (gray bars) cells in the PαS populations.

(G) Numbers of PαS isolated from two limb buds or hindlimb long bones per embryo or mouse shows that PαS cells are most abundant in newborn mice.

All results shown are representative of $n \geq 3$ independent experiments per stage. All results are presented as averages \pm SD in (E–G).

with Figure 4A). Already at this early stage, PαS cells are detected in the developing perichondrium (Figure S2C). Around birth (E18.5 and P2), the CD90^{neg}CD73^{hi} PαS subpopulation is most abundant (Figures 5C and 5F). From W4 onward, the two CD90^{pos} PαS subpopulations become most prominent as they increase to ~75% of all PαS (Figures 5C and 5F). The maximum numbers of PαS cells can be isolated from mouse long bones at early postnatal stages (P1–4: ~12–20 $\times 10^3$ cells), while their numbers decrease progressively thereafter ($\leq 6.5 \times 10^3$ cells in adult mice, Figure 5G). Furthermore, the fraction of Sox9-GFP-positive cells remains rather constant in all four PαS subpopulations

during fetal long bone development, but increases to ~70% by puberty around W4 (Figure 5D).

In Vitro Tri-lineage Differentiation Potential of the Four PαS Subpopulations

As PαS cells are most prominent at P2 (Figure 5G) and the chondrogenic and osteogenic programs are both active, the four subpopulations were isolated from limb long bones to assess their *in vitro* clonogenic and tri-lineage differentiation potential (Figures S3 and 6). Clonal analysis establishes that the clonogenic potential of the two CD90^{pos} subpopulations is ~2-fold higher than one of the CD90^{neg}

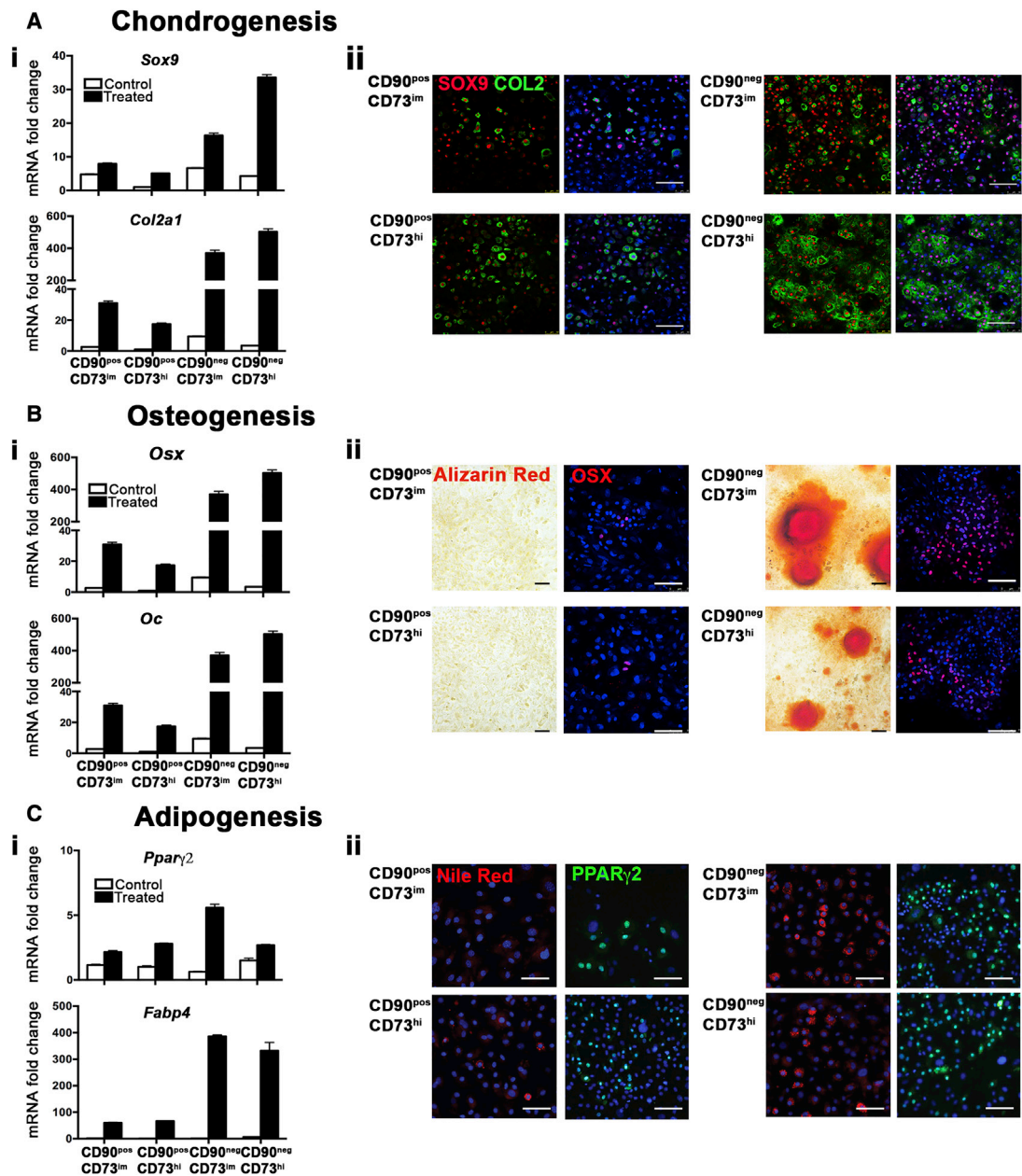


Figure 6. *In Vitro* Tri-lineage Differentiation Potential of the P α S Subpopulations

The four P α S subpopulations were sorted from hindlimb long bones of newborn mice (P2). Cells were briefly expanded and chondrogenic, osteogenic, and adipogenic differentiation using equal numbers of cells from all P α S subpopulations were induced in the appropriate differentiation media. Controls were maintained in expansion medium (see Supplemental Experimental Procedures).

(A) Chondrogenic differentiation was assayed after 5 days: (i) *Sox9* and *Col2a1* transcript levels and (ii) the distribution of SOX9 and collagen type 2 (COL2) proteins are shown.

(B) Osteogenic differentiation was assayed after 21 days. (i) *Osterix* (*Osx*) and *Osteocalcin* (*Oc*) transcript levels. (ii) The extent of mineralization was detected by Alizarin red staining and the OSX protein distribution analyzed by immunofluorescence.

(C) Adipogenic differentiation was analyzed molecularly after 5 days. (i) *Ppar γ 2* and *Fabp4* transcript levels (marking pre-adipocytes and adipocytes). (ii) The peroxisome proliferator-activated receptor γ (PPAR γ) protein distribution was analyzed by immunofluorescence. Lipid droplets were revealed by Nile red staining after 10 days of differentiation.

Transcript levels were normalized to *Rpl-19* transcripts. Nuclei were counterstained with DAPI (blue). $n \geq 2$ independent experiments were analyzed per data point and yielded identical results. Results in (i) are presented as averages \pm SD. Scale bars, 100 μ m.

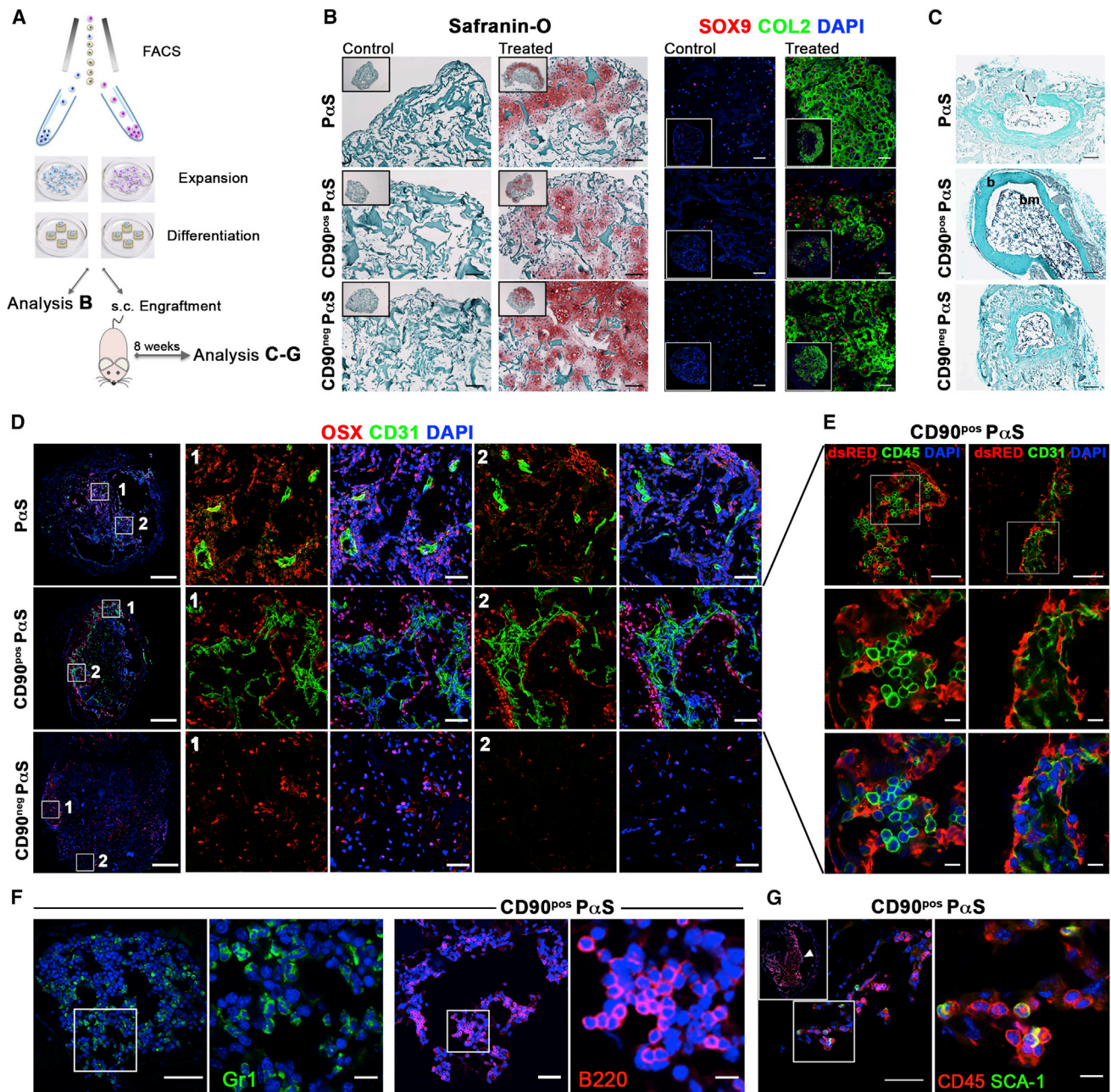


Figure 7. *In Vitro* Chondrogenic and *In Vivo* Bone-Forming Potential of CD90^{pos} and CD90^{neg} P α S Subpopulations

(A) Scheme showing the experimental setup for engraftment of cartilage constructs into nude mice. FACS, fluorescence-activated cell sorting; s.c., subcutaneous.

(B) Total P α S and CD90^{pos} and CD90^{neg} P α S subpopulations were isolated from long bones of newborn mice. Following 1 week of expansion, the different cells were seeded into collagen type 1 (COL1) matrices and cultured for 1 week in chondrogenic differentiation medium (experimental samples) or expansion medium (controls). 3D cartilage constructs were analyzed for morphology (blue) and chondrogenesis by Safranin O (red staining), and the SOX9 (red) and COL2 (green) distribution determined by immunofluorescence. Scale bars, 100 μ m. (C) 3D cartilage constructs were implanted subcutaneously into adult nude mice and retrieved 8 weeks later to assess morphology (blue) and cartilage by Safranin O red staining. Note the absence of cartilage in all samples. No ossicles developed in control implants (see B and data not shown). Frequencies of ossicles with bone structures: P α S constructs n = 5/5; CD90^{pos} P α S constructs n = 5/5; CD90^{neg} P α S constructs n = 2/5. Scale bars, 200 μ m (see also Figure S4).

(legend continued on next page)



P α S subpopulations (Figure S3A). However, cell clones derived from all four P α S subpopulations undergo proliferation arrest during *in vitro* expansion (Figure S3B and data not shown), which precludes generation of sufficient cells for tri-lineage differentiation analysis. Therefore, equal numbers of freshly isolated cells from all four P α S subpopulations were only briefly expanded prior to inducing differentiation into chondrogenic, osteogenic, and adipogenic cells (tri-lineage differentiation, Figure 6; for details see Supplemental Experimental Procedures).

Culturing cells in chondrogenic differentiation medium results in upregulation of *Sox9* and *Col2a* expression in all four P α S subpopulations (Figure 6A). However, the *Sox9* and *Col2a* expression levels are much higher in the two CD90^{neg} P α S subpopulations (CD90^{neg}CD73^{int} and CD90^{neg}CD73^{hi}, Figure 6A). In agreement, the two CD90^{neg} cell populations display a much higher osteogenic and adipogenic differentiation potential than CD90^{pos} cells (Figures 6B and 6C). The *in vitro* tri-lineage differentiation potential of the two CD90^{pos} subpopulations (CD90^{pos}CD73^{hi} and CD90^{pos}CD73^{int}) is lower, but it is important to note that these cells are able to initiate both chondrogenic and adipogenic differentiation programs as revealed by transcriptional upregulation of specific markers for these lineages (Figures 6A and 6C). In osteogenic culture conditions, the *Osx* and *Osteocalcin* (*Oc*) expression is upregulated in both CD90^{pos} subpopulations (Figure 6Bi), but no OSX protein and mineralization (visualized by Alizarin red staining) are detected (Figure 6Bii). These results indicate that while the CD90^{neg} P α S cells possess robust tri-lineage differentiation potential upon induction in culture, the CD90^{pos} P α S cells initiate differentiation along all three lineages but fail to undergo complete adipogenic and osteogenic differentiation in 2D cultures (Figure 6).

Cartilage Derived from CD90^{pos} P α S Cells Is Remodeled *In Vivo* into Bone Organoids Attracting Host-Derived Angiogenesis and Hematopoiesis

The *in vivo* differentiation and endochondral-bone-forming potential of CD90^{neg} and CD90^{pos} P α S cells isolated

from newborn mice was assayed by subcutaneous engraftment of engineered 3D cartilage tissue implanted into nude mice (Figure 7). These two rather than all four P α S subpopulations were assayed, as the respective *in vitro* differentiation of the two CD90^{neg} and two CD90^{pos} subpopulations is very similar (Figure 6). Following flow-cytometric isolation of parental P α S cells and its CD90^{neg} and CD90^{pos} subpopulations, cells were briefly expanded, seeded into collagen type 1 (COL1) matrices, and cultured in chondrogenic medium (Figure 6A, see Experimental Procedures). After 1 week, the cartilage scaffolds generated by the three different cell populations were either analyzed (Figure 7B) or implanted subcutaneously into athymic nude mice (Figure 7C).

Safranin O staining of matrices and detection of the SOX9 and COL2 proteins after 2 weeks showed that all three cell populations are able to produce cartilage in COL1 matrices (Figure 7B). In particular, it appears that the chondrogenic differentiation potential of CD90^{pos} P α S cells is significantly enhanced by culturing them in 3D COL1 matrices (Figure 7B, compare with Figure 6Aii).

Eight weeks after subcutaneous implantation, the three types of scaffolds were explanted and histological analysis established that all cartilage tissues engineered from parental P α S cells and the CD90^{pos} P α S subpopulation had formed ossicles with bone marrow cavities ($n = 5/5$, Figure 7C). In contrast, bone formation by CD90^{neg} P α S-based constructs is less efficient, as small ossicles with a poorly developed bone marrow compartment formed in only two of the five implants (Figure 7C). The absence of glycosaminoglycans (normally stained in red by Safranin O) establishes that the cartilage extracellular matrix was not maintained *in vivo*. Indeed, neither COL2 nor Aggrecan were detected in the remodeled explants (data not shown). As a significant fraction of P α S cells comprises SOX9-positive cells (Figure 5D), we analyzed the SOX9 distribution in the explants by immunofluorescence (Figure S4). Few scattered SOX9-positive cells are present in explants derived from P α S cells and

(D) Immunofluorescence analysis of the different constructs after 8 weeks *in vivo* differentiation to detect OSX-positive cells (red) and CD31-positive endothelial cells (green, indicative of angiogenesis). Sections were counterstained with DAPI (blue) to reveal nuclei. The enlarged regions 1 and 2 are shown in the right panels. Scale bars, 500 μ m (low magnification) and 100 μ m (high magnification).

(E) Immunofluorescence analysis of ossicles retrieved after implanting DsRed-positive CD90^{pos} P α S cartilage constructs (8 weeks). Left panels show that the CD45-positive hematopoietic cells are host derived, as they are not expressing DsRed. Right panels show that the CD31-positive endothelial cells are also host derived. Scale bars, 100 μ m (upper panels) and 10 μ m (middle and lower panels).

(F) Sections through the bone marrow of CD90^{pos}P α S ossicles. Immunofluorescence analysis reveals Gr1-positive granulocytes and B220-positive cells (immature and mature B lymphocytes). Nuclei were counterstained with DAPI (blue). Scale bars, 100 μ m (low magnification) and 10 μ m (high magnification).

(G) Co-localization of CD45 and SCA-1 (yellow) labels HSCs and multipotent progenitors. Co-expressing cells were observed near the endosteum (arrowhead in the left panel). Nuclei were stained with DAPI. Scale bars, 100 μ m (low magnification) and 10 μ m (high magnification).

All results are representative of $n \geq 3$ independent samples.



CD90^{pos}P α S chondrogenic scaffolds, while abundant SOX9-positive cells remain in CD90^{neg} P α S explants (Figure S4). In fact, this analysis showed that cartilage was not maintained in any of the constructs generated using the three different cell populations. This is likely due to the fact that the milieu of the host does not support cartilage maintenance, which depends on inhibition of VEGF signaling (Chan et al., 2015).

The distribution of CD31-positive endothelial and OSX-positive cells (Maes et al., 2010; Ono et al., 2014a) was analyzed on sections to gain insight into the extent to which the endochondral ossification had processed (Figure 7D). Cells expressing these markers are abundant in both P α S cells and CD90^{pos} P α S ossicles, but the distribution of CD31-positive and OSX-positive cells is much more organized in ossicles derived from CD90^{pos} P α S than in the ones using unfractionated P α S (Figure 7D). This correlates well with the larger and well-structured bone marrow compartment observed in CD90^{pos} P α S ossicles, which are reminiscent of bone organoids (Figure 7C). In contrast, fewer OSX-positive and no CD31-positive cells are detected in CD90^{neg} P α S explants (Figure 7D). These observations, together with the presence of a large number of SOX9-positive cells (Figure S4), suggests that endochondral ossification was arrested at an early step during remodeling of CD90^{pos} P α S implants.

To determine whether the endothelial and OSX-positive cells were derived from implant or host, we isolated CD90^{pos} P α S cells from newborn mice expressing DsRed ubiquitously (Vintersten et al., 2004) and used them to generate cartilage constructs for implantation (Figure 7A). After 8 weeks, explants were analyzed by immunofluorescence. Donor-derived DsRed-positive cells are located in the compact bone and in the bone marrow in close contact with host-derived endothelial and hematopoietic cells (Figure 7E). In contrast, all hematopoietic (CD45) and endothelial (CD31) cells lack DsRed, which establishes that they are recruited from the host (Figure 7E). Further analysis of the hematopoietic compartment showed that CD45^{pos} cells encompass descendants of the common myeloid (granulocytes Gr1^{pos}) and common lymphoid progenitors (immature and mature B cells detected by B220, Figure 7F). Rare CD45 SCA-1 double-positive cells are detected near the endosteum, which is indicative of multipotent hematopoietic progenitors (Seita and Weissman, 2010). Our results establish that expanding P α S CD90^{pos} shortly in culture and differentiating them in 3D COL1 matrices results in cartilage constructs that are very efficiently remodeled into bone organoids *in vivo* (Figure 7C). In particular, the engrafted constructs attract host-derived endothelial cells to establish angiogenesis and generate a niche to recruit and

maintain host-derived multipotent HSCs for hematopoiesis (Figures 7D–7G).

DISCUSSION

Flow-cytometric analysis was used to study the ontogeny of different mesenchymal progenitor populations during mouse limb and long bone development and homeostasis. We show that the majority of Lin^{neg} mesenchymal cells during embryonic limb and fetal long bone are P α CD51 cells (Pinho et al., 2013), while their numbers drop drastically after birth. A small fraction of *Prx1*-expressing P α CD51 cells persists into adulthood. This is in support of P α CD51 cells retaining progenitor characteristics. Most importantly, P α CD51 cells encompass at least three distinct cell populations: P α S cells (Morikawa et al., 2009), CD200^{pos} cells that contain all mSSCs (Chan et al., 2015), and at least one additional population, SCA-1^{neg}CD200^{neg} P α CD51 cells. These P α CD51DN cells express the highest levels of *Cxcl12*, which indicates that they might encompass/correspond to the adipo-osteogenic CAR progenitors needed for maturation of B lymphocytes (Greenbaum et al., 2013; Omatsu et al., 2010; Sugiyama et al., 2006). This is in line with the recent observation that CAR cells are derived from the P α S population (Hu et al., 2016) and the fact that human P α CD51 cells isolated from fetal bone marrow are self-renewing, possess multilineage potential, and provide HSC niche functions (Pinho et al., 2013). In addition, the different mesenchymal cell populations express *Lepr*, which is interesting as *Lepr*-positive mesenchymal progenitors are a main source of bone formed by adult bone marrow (Zhou et al., 2014a). Finally, we show that the most abundant stromal cells from adult bones are P α cells. However, as these P α -positive cells neither express *Prx1* nor any of the other osteo-chondrogenic markers analyzed in a robust manner, they likely correspond to fibroblasts given their poor survival in culture (G.N. and R.Z., unpublished data).

Our results establish the SCA-1^{pos} P α S and the CD200^{pos} mSSCs are mutually exclusive mesenchymal progenitors with distinct developmental origins. Within the P α CD51 mesenchymal progenitors, SCA-1^{pos} cells are detected much earlier than CD200^{pos} cells in mouse limb buds. Others have proposed that the CD200^{pos} mSSCs are related to the progenitors that participate in endochondral bone formation during limb bud development, postnatal bone growth, and fracture healing (Cervantes-Diaz et al., 2016; Chan et al., 2015; Serafini et al., 2014; Yang et al., 2014; Zhou et al., 2014b). In contrast, the *Sca-1*-expressing mesenchymal progenitors are detected in early limb buds surrounding the chondrogenic anlagen. Contrary to bulk of limb bud mesenchymal progenitors, SCA-1^{pos} cells are



not significantly expanded prior to the onset of endochondral ossification (G.N. and R.Z., unpublished data). After birth, P α S cells continue to express *Prx1* and low levels of *Cxcl12* and *LepR*, but not *Col2a1*, *Mmp13*, and *Osx* (Greenbaum et al., 2013; Morikawa et al., 2009; Ono et al., 2014b). At this stage it is unclear whether the SCA-1^{POS} progenitors present in early mouse limb buds give rise to definitive P α S cells.

We also show that P α S cells are not homogeneous, but consist of four subpopulations that become apparent during the onset of endochondral ossification. The highest numbers of P α S cells are detected perinatally and in newborn mice; coinciding with abundant chondrogenic and osteogenic activity, peak of endothelial cell numbers, and migration of fetal HSCs from liver to bone marrow (Ono et al., 2014a; Trumpp et al., 2010). While all four subpopulations display CFU-F frequencies similar to that of the parental P α S population (Morikawa et al., 2009), they cannot be extensively expanded in culture (this study). In agreement with the major chondrogenic activity during embryonic and early postnatal long bone development, the two CD90^{NEG} subpopulations represent the bulk of P α S cells during this period and possess the best tri-lineage differentiation potential *in vitro*. Therefore, it was unexpected that CD90^{NEG} P α S cartilage constructs are not remodeled into bone organoids, but appear arrested at an early stage. This suggests that 3D cartilage constructs generated from CD90^{NEG} P α S either lack osteogenic progenitors and/or that chondrogenesis did not progress to hypertrophy, which is necessary to trigger endochondral ossification (Long and Ornitz, 2013).

The ratio between CD90^{NEG} and CD90^{POS} cells reverses in long bones around 2 weeks after birth as the CD90^{POS} P α S subpopulation becomes predominant. This switch occurs as the migration of HSCs is complete and bone marrow homeostasis is achieved (Trumpp et al., 2010). CD90^{POS} P α S cells initiate, but do not complete tri-lineage differentiation in 2D culture, while seeding into 3D COL1 matrices results in efficient cartilage production. Most strikingly, CD90^{POS} P α S cells have the highest CFU-F potential in culture, and cartilage constructs derived from these cells are efficiently remodeled into bone organoids *in vivo*. These bone organoids contain a well-structured marrow with a host-derived hematopoietic and vascular system. In particular, donor-derived OSX^{POS} cells resembling perinatal mesenchymal stromal progenitors (Liu et al., 2013; Maes et al., 2010; Mizoguchi et al., 2014; Ono et al., 2014b) are present in proximity to host-derived endothelial and hematopoietic cells. Most importantly, rare CD45^{POS}SCA-1^{POS} cells are detected close to the endosteum, indicating that they correspond to short-term self-renewing HSCs. These findings agree with previous studies showing that P α S cells are required to maintain long-term self-renewing

HSCs (Greenbaum et al., 2013; Hu et al., 2016; Morikawa et al., 2009).

Our study defines the emergence and relationships among the most relevant MSC-like populations in mice. In addition, we identify distinct P α S subpopulations and show that one of them, the CD90^{POS} P α S subpopulation, has the potential to differentiate into cartilage that is remodeled into bone organoids with a functional marrow in mice. As mouse P α S cells are contained within the P α CD51 population, our study could pave the way to identify the orthologous cells in humans, which may have important therapeutic implications for cartilage and bone tissue engineering and their co-transplantation with HSCs in human patients.

EXPERIMENTAL PROCEDURES

A detailed description of all procedures is included in [Supplemental Experimental Procedures](#).

Mouse Strains

All studies using mice were performed strictly in adherence with Swiss law, the 3R principles, and the Basel Declaration. All animal studies were approved by the cantonal animal welfare and ethics committee (licenses no. 1951 to R.Z. and no. 1797 to I.M.). Personnel performing animal studies are trained and licensed according to FELASA standards. The persons performing surgery (subcutaneous implantation) have been specially trained. Unless indicated otherwise, mice of both sexes were used for analysis. The *Prx1*-Cre (Logan et al., 2002), DsRed (mouse strain generated using DsRed.T3-expressing embryonic stem cells; Vintersten et al., 2004), inducible β -Act-GFP (Jagle et al., 2007), and Sox9^{IRRES-EGFP} (Sox9-GFP, Chan et al., 2011) mouse strains were kept in a C57BL/6J genetic background. C57BL/6 and CD1 nude mice were purchased from Janvier and Charles River Laboratories, respectively.

Isolation of Mesenchymal Cells from Limb Buds and Long Bones for Flow-Cytometric Analysis

Cell suspensions were prepared from mouse embryonic limb buds and long bones for flow-cytometry analysis and sorting as described by Houlihan et al. (2012). The modifications necessary to adapt the protocol to the different developmental stages analyzed are described in [Supplemental Experimental Procedures](#).

Subcutaneous Engraftment of 3D Cartilage Scaffolds

P α S and CD90^{POS} and CD90^{NEG}P α S subpopulations were sorted by flow cytometry from mouse hindlimb long bones at postnatal day 2 (P2) and expanded *in vitro* for 5–7 days under normoxic conditions (21% O₂, 5% CO₂; [Supplemental Experimental Procedures](#)). Then 100,000 cells (20,000 cells/ μ L) were seeded per COL1-matrix (Avitene Ultrafoam Collagen Sponge; C.R. Bard, USA) and cultured in expansion medium overnight. Half of the matrices were continuously cultured in expansion medium to serve as controls, while the others were cultured in chondrogenic



differentiation medium for 7 days (Supplemental Experimental Procedures). After this, one set of COL1-constructs per cell type was used for histological analysis by Von Kossa staining, Safranin O staining, and immunofluorescence. The others were subcutaneously implanted into adult nude CD1 mice (weeks 12–15) as previously described (Scotti et al., 2010). Constructs were retrieved 8 weeks later and analyzed by histology and immunofluorescence (Supplemental Experimental Procedures and Scotti et al., 2013).

SUPPLEMENTAL INFORMATION

Supplemental Information includes Supplemental Experimental Procedures and four figures and can be found with this article online at <http://dx.doi.org/10.1016/j.stemcr.2017.08.007>.

AUTHOR CONTRIBUTIONS

G.N and S.J. performed all the flow-cytometric studies and most of the other analysis. R.R. performed the *in situ* hybridization. A.B. and A.H. performed the implantation studies in nude mice, and the analysis was done together with S.J. and G.N. Adipogenic differentiation assays were performed by D.I.R. and S.J., and T.L. provided the Sox9^{IRESGFP} (Sox9-GFP) mice generated in his group prior to publication. R.Z., I.M., and G.N. conceived and supervised the studies. I.M. and R.Z. acquired the necessary funding. R.Z. and G.N. wrote the manuscript with input from all authors.

ACKNOWLEDGMENTS

The authors wish to thank A. Brühlhard and his team for excellent animal care; A. Todorov for help in performing the surgery in mice; and P. Lorentz from the DBM Microscopic Core facility for his assistance. We are indebted to G. Christofori for input and support concerning the adipogenesis analysis. We thank members of the Developmental Genetics and Tissue Engineering groups for critical input into the study and manuscript. This study is supported by SNF grants (Sinergia CRSII3_136179 and research grant 31003A_156430) awarded jointly to I.M. and R.Z. R.R. is the recipient of a postdoctoral fellowship award by the DFG. Additional core funding was provided by the University of Basel and the University Hospital of Basel. The authors dedicate this publication to the memory of Ton Rolink, who was key for initiating the study and whose passion for science will continue to inspire us.

Received: January 27, 2017

Revised: August 14, 2017

Accepted: August 14, 2017

Published: September 14, 2017

REFERENCES

Akiyama, H., Chaboissier, M.C., Martin, J.F., Schedl, A., and de Crombrughe, B. (2002). The transcription factor Sox9 has essential roles in successive steps of the chondrocyte differentiation pathway and is required for expression of Sox5 and Sox6. *Genes Dev.* 16, 2813–2828.

Akiyama, H., Kim, J.E., Nakashima, K., Balmes, G., Iwai, N., Deng, J.M., Zhang, Z., Martin, J.F., Behringer, R.R., Nakamura, T., et al.

(2005). Osteo-chondroprogenitor cells are derived from Sox9 expressing precursors. *Proc. Natl. Acad. Sci. USA* 102, 14665–14670.

Akiyama, H., and Lefebvre, V. (2011). Unraveling the transcriptional regulatory machinery in chondrogenesis. *J. Bone Miner Metab.* 29, 390–395.

Bianco, P. (2014). “Mesenchymal” stem cells. *Annu. Rev. Cell Dev. Biol.* 30, 677–704.

Caplan, A.I. (2017). Mesenchymal stem cells: time to change the name!. *Stem Cells Trans Med* 6, 1445–1451.

Cervantes-Diaz, F., Contreras, P., and Marcellini, S. (2016). Evolutionary origin of endochondral ossification: the transdifferentiation hypothesis. *Dev. Genes Evol.* 227, 121–127.

Chan, C.K., Chen, C.C., Luppen, C.A., Kim, J.B., DeBoer, A.T., Wei, K., Helms, J.A., Kuo, C.J., Kraft, D.L., and Weissman, I.L. (2009). Endochondral ossification is required for haematopoietic stem-cell niche formation. *Nature* 457, 490–494.

Chan, C.K., Seo, E.Y., Chen, J.Y., Lo, D., McArdle, A., Sinha, R., Tevlin, R., Seita, J., Vincent-Tompkins, J., Wearda, T., et al. (2015). Identification and specification of the mouse skeletal stem cell. *Cell* 160, 285–298.

Chan, H.Y., Sivakamasundari, V., Xing, X., Kraus, P., Yap, S.P., Ng, P., Lim, S.L., and Lufkin, T. (2011). Comparison of IRES and F2A-based locus-specific multicistronic expression in stable mouse lines. *PLoS One* 6, e28885.

Chitteti, B.R., Cheng, Y.H., Kacena, M.A., and Srour, E.F. (2013). Hierarchical organization of osteoblasts reveals the significant role of CD166 in hematopoietic stem cell maintenance and function. *Bone* 54, 58–67.

Chung, M.T., Liu, C., Hyun, J.S., Lo, D.D., Montoro, D.T., Hasegawa, M., Li, S., Sorkin, M., Rennert, R., Keeney, M., et al. (2013). CD90 (Thy-1)-positive selection enhances osteogenic capacity of human adipose-derived stromal cells. *Tissue Eng. Part A* 19, 989–997.

Dy, P., Wang, W., Bhattaram, P., Wang, Q., Wang, L., Ballock, R.T., and Lefebvre, V. (2012). Sox9 directs hypertrophic maturation and blocks osteoblast differentiation of growth plate chondrocytes. *Dev. Cell* 22, 597–609.

Greenbaum, A., Hsu, Y.M., Day, R.B., Schuettelpelz, L.G., Christopher, M.J., Borgerding, J.N., Nagasawa, T., and Link, D.C. (2013). CXCL12 in early mesenchymal progenitors is required for haematopoietic stem-cell maintenance. *Nature* 495, 227–230.

Houlihan, D.D., Mabuchi, Y., Morikawa, S., Niibe, K., Araki, D., Suzuki, S., Okano, H., and Matsuzaki, Y. (2012). Isolation of mouse mesenchymal stem cells on the basis of expression of Sca-1 and PDGFR-alpha. *Nat. Protoc.* 7, 2103–2111.

Hu, X., Garcia, M., Weng, L., Jung, X., Murakami, J.L., Kumar, B., Warden, C.D., Todorov, I., and Chen, C.C. (2016). Identification of a common mesenchymal stromal progenitor for the adult haematopoietic niche. *Nat. Commun.* 7, 13095.

Jagle, U., Gasser, J.A., Muller, M., and Kinzel, B. (2007). Conditional transgene expression mediated by the mouse beta-actin locus. *Genesis* 45, 659–666.

Kim, I., Saunders, T.L., and Morrison, S.J. (2007). Sox17 dependence distinguishes the transcriptional regulation of fetal from adult hematopoietic stem cells. *Cell* 130, 470–483.



- Lee, P.Y., Wang, J.X., Parisini, E., Dascher, C.C., and Nigrovic, P.A. (2013). Ly6 family proteins in neutrophil biology. *J. Leukoc. Biol.* *94*, 585–594.
- Liu, Y., Strecker, S., Wang, L., Kronenberg, M.S., Wang, W., Rowe, D.W., and Maye, P. (2013). Osterix-cre labeled progenitor cells contribute to the formation and maintenance of the bone marrow stroma. *PLoS One* *8*, e71318.
- Logan, M., Martin, J.F., Nagy, A., Lobe, C., Olson, E.N., and Tabin, C.J. (2002). Expression of Cre Recombinase in the developing mouse limb bud driven by a Pxl enhancer. *Genesis* *33*, 77–80.
- Long, F., and Ornitz, D.M. (2013). Development of the endochondral skeleton. *Cold Spring Harb Perspect. Biol.* *5*, a008334.
- Mabuchi, Y., Houlihan, D.D., Akazawa, C., Okano, H., and Matsuzaki, Y. (2013). Prospective isolation of murine and human bone marrow mesenchymal stem cells based on surface markers. *Stem Cells Int.* *2013*, 7.
- Maes, C., Kobayashi, T., Selig, M.K., Torrekens, S., Roth, S.I., Mackem, S., Carmeliet, G., and Kronenberg, H.M. (2010). Osteoblast precursors, but not mature osteoblasts, move into developing and fractured bones along with invading blood vessels. *Dev. Cell* *19*, 329–344.
- Mizoguchi, T., Pinho, S., Ahmed, J., Kunisaki, Y., Hanoun, M., Mendelson, A., Ono, N., Kronenberg, H.M., and Frenette, P.S. (2014). Osterix marks distinct waves of primitive and definitive stromal progenitors during bone marrow development. *Dev. Cell* *29*, 340–349.
- Morikawa, S., Mabuchi, Y., Kubota, Y., Nagai, Y., Niibe, K., Hiratsu, E., Suzuki, S., Miyauchi-Hara, C., Nagoshi, N., Sunabori, T., et al. (2009). Prospective identification, isolation, and systemic transplantation of multipotent mesenchymal stem cells in murine bone marrow. *J. Exp. Med.* *206*, 2483–2496.
- Morrison, S.J., and Scadden, D.T. (2014). The bone marrow niche for haematopoietic stem cells. *Nature* *505*, 327–334.
- Ode, A., Schoon, J., Kurtz, A., Gaetjen, M., Ode, J.E., Geissler, S., and Duda, G.N. (2013). CD73/5'-ecto-nucleotidase acts as a regulatory factor in osteo-/chondrogenic differentiation of mechanically stimulated mesenchymal stromal cells. *Eur. Cell Mater* *25*, 37–47.
- Omatsu, Y., Sugiyama, T., Kohara, H., Kondoh, G., Fujii, N., Kohno, K., and Nagasawa, T. (2010). The essential functions of adipo-osteogenic progenitors as the hematopoietic stem and progenitor cell niche. *Immunity* *33*, 387–399.
- Ono, N., and Kronenberg, H.M. (2016). Bone repair and stem cells. *Curr. Opin. Genet. Dev.* *40*, 103–107.
- Ono, N., Ono, W., Mizoguchi, T., Nagasawa, T., Frenette, P.S., and Kronenberg, H.M. (2014a). Vasculature-associated cells expressing nestin in developing bones encompass early cells in the osteoblast and endothelial lineage. *Dev. Cell* *29*, 330–339.
- Ono, N., Ono, W., Nagasawa, T., and Kronenberg, H.M. (2014b). A subset of chondrogenic cells provides early mesenchymal progenitors in growing bones. *Nat. Cell Biol* *16*, 1157–1167.
- Park, D., Spencer, J.A., Koh, B.I., Kobayashi, T., Fujisaki, J., Clemens, T.L., Lin, C.P., Kronenberg, H.M., and Scadden, D.T. (2012). Endogenous bone marrow MSCs are dynamic, fate-restricted participants in bone maintenance and regeneration. *Cell Stem Cell* *10*, 259–272.
- Pinho, S., Lacombe, J., Hanoun, M., Mizoguchi, T., Bruns, I., Kunisaki, Y., and Frenette, P.S. (2013). PDGFRalpha and CD51 mark human nestin+ sphere-forming mesenchymal stem cells capable of hematopoietic progenitor cell expansion. *J. Exp. Med.* *210*, 1351–1367.
- Sacchetti, B., Funari, A., Michienzi, S., Di Cesare, S., Piersanti, S., Saggio, I., Tagliafico, E., Ferrari, S., Robey, P.G., Riminucci, M., et al. (2007). Self-renewing osteoprogenitors in bone marrow sinusoids can organize a hematopoietic microenvironment. *Cell* *131*, 324–336.
- Scotti, C., Piccinini, E., Takizawa, H., Todorov, A., Bourguine, P., Papadimitropoulos, A., Barbero, A., Manz, M.G., and Martin, I. (2013). Engineering of a functional bone organ through endochondral ossification. *Proc. Natl. Acad. Sci. USA* *110*, 3997–4002.
- Scotti, C., Tonnarelli, B., Papadimitropoulos, A., Scherberich, A., Schaeren, S., Schauerte, A., Lopez-Rios, J., Zeller, R., Barbero, A., and Martin, I. (2010). Recapitulation of endochondral bone formation using human adult mesenchymal stem cells as a paradigm for developmental engineering. *Proc. Natl. Acad. Sci. USA* *107*, 7251–7256.
- Seita, J., and Weissman, I.L. (2010). Hematopoietic stem cell: self-renewal versus differentiation. *WIREs Syst. Biol. Med.* *2*, 640–653.
- Serafini, M., Sacchetti, B., Pievani, A., Redaelli, D., Remoli, C., Biondi, A., Riminucci, M., and Bianco, P. (2014). Establishment of bone marrow and hematopoietic niches in vivo by reversion of chondrocyte differentiation of human bone marrow stromal cells. *Stem Cell Res* *12*, 659–672.
- Sugiyama, T., Kohara, H., Noda, M., and Nagasawa, T. (2006). Maintenance of the hematopoietic stem cell pool by CXCL12-CXCR4 chemokine signaling in bone marrow stromal cell niches. *Immunity* *25*, 977–988.
- ten Berge, D., Brugmann, S.A., Helms, J.A., and Nusse, R. (2008). Wnt and FGF signals interact to coordinate growth with cell fate specification during limb development. *Development* *135*, 3247–3257.
- Trumpp, A., Essers, M., and Wilson, A. (2010). Awakening dormant haematopoietic stem cells. *Nat. Rev. Immunol.* *10*, 201–209.
- Vintersten, K., Monetti, C., Gertsenstein, M., Zhang, P., Laszlo, L., Biechele, S., and Nagy, A. (2004). Mouse in red: red fluorescent protein expression in mouse ES cells, embryos, and adult animals. *Genesis* *40*, 241–246.
- Wu, L., Bluggermann, C., Kyupelyan, L., Latour, B., Gonzalez, S., Shah, S., Galic, Z., Ge, S., Zhu, Y., Petrigliano, F.A., et al. (2013). Human developmental chondrogenesis as a basis for engineering chondrocytes from pluripotent stem cells. *Stem Cell Rep.* *1*, 575–589.
- Yang, L., Tsang, K.Y., Tang, H.C., Chan, D., and Cheah, K.S. (2014). Hypertrophic chondrocytes can become osteoblasts and osteocytes in endochondral bone formation. *Proc. Natl. Acad. Sci. USA* *111*, 12097–12102.
- Zhou, B.O., Yue, R., Murphy, M.M., Peyer, J.G., and Morrison, S.J. (2014a). Leptin-receptor-expressing mesenchymal stromal cells represent the main source of bone formed by adult bone marrow. *Cell Stem Cell* *15*, 154–168.
- Zhou, X., von der Mark, K., Henry, S., Norton, W., Adams, H., and de Crombrughe, B. (2014b). Chondrocytes transdifferentiate into osteoblasts in endochondral bone during development, postnatal growth and fracture healing in mice. *PLoS Genet.* *10*, e1004820.